Surface-Induced Nickel Hydroxide Precipitation in the Presence of Citrate and Salicylate

Noriko U. Yamaguchi,* Andreas C. Scheinost, and Donald L. Sparks

ABSTRACT

Formation of surface-induced precipitates may play an important role in the immobilization of Ni and other metals in nonacidic soils. To investigate the influence of commonly present organic ligands on precipitate formation, we monitored the uptake of Ni by gibbsite and pyrophyllite in the presence of citrate and salicylate for 4 wk and identified the Ni hydroxide precipitates with diffuse reflectance spectroscopy (DRS). In the absence of organic ligands, Ni uptake proceeded by formation of Ni–Al layered double hydroxide (LDH) precipitates. Citrate and salicylate generally decreased both the Ni removal from solution and the precipitate formation. The suppression by citrate was more pronounced than that by salicylate due to the stronger complexation of Ni by citrate. In the presence of citrate and salicylate, the precipitate phase was Ni–Al LDH on pyrophyllite, but predominately α-Ni hydroxide on gibbsite. This difference can be explained by the differing Al solubilities of the two minerals. Pyrophyllite is relatively soluble, causing the rapid formation of amorphous Al hydroxide, which, in turn, is a necessary precursor for the formation of Ni–Al LDH. In spite of the complexation of Al by organic ligands, sufficient amorphous Al hydroxide was available to promote the formation of Ni–Al LDH. Gibbsite, on the other hand, is much less soluble, and the smaller amount of initially released Al may be fully complexed by citrate and salicylate. The subsequent lack of amorphous Al hydroxide prevented the formation of Ni–Al LDH, and, instead, α-Ni hydroxide formed. Only after a longer period of 30 d and at a low citrate concentration did enough Al become available to transform α-Ni hydroxide into the thermodynamically more stable Ni–Al LDH.

Nickel contamination of soils is a serious problem as a result of industrial and mining activities. Since Ni is highly toxic to plants and animals, its fate and mobility in soils are of great concern. The sorption of Ni onto soil surfaces controls the Ni distribution in soil and aquatic system. Therefore, identification of sorption mechanisms is a prerequisite to establish risk assessment and remediation strategies for Ni contaminated soils. Many attempts have been made towards that goal using binary sorbent–sorbate systems and spectroscopic techniques. However, the fate of metals in soils may differ from that predicted by such relatively simple laboratory experiments because of the presence of a variety of inorganic and organic ions in soil solution. Organic ligands are of special interest since they are exuded into the soil solution by plants, fungi, and microorganisms (Strom, 1997), and since they may enhance the solubility and mobility of metals (Gadd, 1999; Jones, 1998).

N.U. Yamaguchi, Dep. of Biological and Environmental Engineering, Graduate School of Agricultural and Life Sciences, The University of Tokyo, 1-1-1 Yayoi, Bunkyo, Tokyo, 113-8657, Japan; A.C. Scheinost, Inst. of Terrestrial Ecology, ETHZ, CH-8952 Schlieren, Switzerland; and D.L. Sparks, Dep. of Plant and Soil Sciences, University of Delaware, Newark, DE 19717-1303. Received 3 Feb. 2000. *Corresponding author (noriko@soil.en.a.u-tokyo.ac.jp).

Published in Soil Sci. Soc. Am. J. 65:729–736 (2001).

X-ray absorption spectroscopy (XAS) studies revealed that Ni(II), Co(II), and Zn(II) formed LDH precipitates on Al-bearing minerals and in soil at pH ≥ 7 (d'Espinose de la Caillerie et al., 1995; Towle et al., 1997; Scheidegger et al., 1997; Scheidegger et al., 1998; Roberts et al., 1999; Ford and Sparks, 2000). These LDH phases consist of brucite-type mixed-metal hydroxide sheets, which are separated from each other by water and charge-balancing anions. Their formula is $[M^{2+}_{1-x}Al^{3+}_{x}(OH)_2]^{x+}\ (x/n)A^{-n}\ mH_2O$, where M^{2+} represents a range of transition metals. The net positive layer charge is balanced by anions such as NO_3^-, Cl^-, CO_3^{2-}, and ClO_4^- (A^{-n}) (Hashi et al., 1983; Génin et al., 1991). In the presence of Al-free minerals, structurally very similar but thermodynamically less stable α-type metal hydroxides with the formula $M(OH)_{2-x}\ (x/n)A^{-n}mH_2O$ have been identified by DRS and XAS (Scheinost et al., 1999; Scheinost and Sparks, 2000). Both types of precipitates create a sink for Ni and are more stable than Ni bound as outer-sphere or inner-sphere sorption complexes (Bradbury and Baeyens, 1997). However, Ni–Al LDH is more resistant to dissolution than α-Ni hydroxide. (Scheckel et al., 2000). Therefore, to accurately predict the fate of Ni in soils and sediments, it is important to understand the controls for the formation of specific precipitates.

Scheidegger et al. (1998) suggested that the rate-limiting step for the formation of Ni–Al LDH is Al dissolution from the mineral surface. This is in consistent with the observation that Ni–Al LDH formed after only 5 min in the presence of the relatively soluble pyrophyllite, but only after 24 h in the presence of the more stable gibbsite (Scheinost et al., 1999). In both cases, dissolution of the mineral surfaces may be enhanced by Ni-promoted dissolution (d'Espinose de la Caillerie et al., 1995). Evidence for pyrophyllite dissolution was suggested by increasing Si concentrations in solution. However, the Al concentrations in gibbsite and pyrophyllite systems remained below 1 μmol L^{-1}, most likely due to precipitation of amorphous Al hydroxide (Thompson et al., 1999). Together with an initial Ni hydroxide phase, the Al hydroxide is a necessary precursor for the formation of Ni–Al LDH (Boclair and Braterman, 1999; Taylor, 1984). The progression of the dissolution explains the constant growth of Ni–Al LDH, which has been observed as long as sufficient Ni was in solution (Scheinost et al., 1999).

Organic ligands form complexes with both surface-bound and aqueous cations. Depending on pH, and type and concentration of organic ligands, mineral dissolu-

Abbreviations: DRS, diffuse reflectance spectroscopy; HS-gibbsite, high surface area gibbsite; LDH, layered double hydroxide; LS-gibbsite, low surface area gibbsite; PZSE, point of zero salt effect; XAS, x-ray absorption spectroscopy.

tion may or may not be enhanced (Drever and Stillings, 1997; Kraemer et al., 1998), and metal adsorption by mineral surfaces may be suppressed or enhanced by the presence of ligands (Brooks and Herman, 1998; Bryce et al., 1994; Boily and Fein, 1996). Consequently, organic ligands may affect the formation process of Ni–Al LDH and α-Ni hydroxide.

In this context, we used citrate and salicylate as representatives of tricarboxylic and monocarboxylic ligands in soils (Tan, 1986) and investigated their influence on the formation of surface-induced Ni hydroxides. Our working hypothesis was that they may affect the precipitate formation by two main processes:

1. The formation of aqueous complexes with Ni and Al may reduce the formation of precipitates in general, and may enhance the relative amount of α-Ni hydroxide.
2. The ligand-enhanced dissolution of the sorbent phases enhances the availability of Al; hence, the precipitation of Ni–Al LDH may be favored.

Pyrophyllite and gibbsite were chosen as sorbents because of their differing stability towards Al release. To monitor precipitate formation we used DRS, which is capable of detecting and discriminating Ni–Al LDH and α-Ni hydroxide (Scheinost et al., 1999).

MATERIALS AND METHODS

Sorbents

Three Al-bearing minerals, low surface area gibbsite (LS-gibbsite) with a specific surface area of 25 $m^2\ g^{-1}$, high surface area gibbsite (HS-gibbsite, 96 $m^2\ g^{-1}$), and pyrophyllite (95 $m^2\ g^{-1}$), were used in this study. The HS-gibbsite was synthesized by the method of Kyle et al. (1975). We slowly added a 4 *M* NaOH to 1 *M* $AlCl_3$ to reach a constant pH of 4.6. The gelatinous precipitate was transferred into cellulose dialysis membrane tubes (Spectra/Por, Spectrum Laboratories, Rancho Dominguez, CA; molecular weight cut off: 12 000–14 000) and dialyzed against deionized water for 36 d. The precipitate was pure gibbsite as verified by x-ray diffraction and infrared spectroscopy. The preparation and characterization of LS-gibbsite and of pyrophyllite are described elsewhere (Scheidegger et al., 1996). The point of zero salt effect (PZSE) was determined according to Method I of Schulthess and Sparks (1986) as the cross-sectional point of pH vs. initial proton concentration curves at three different ionic strengths. The sorbent materials were equilibrated for 24 h with various concentrations of $HClO_4$ and NaOH solutions at ionic strengths of 0.01, 0.1, and 1 *M*. The PZSE of LS-gibbsite, HS-gibbsite, and pyrophyllite was 9.0, 10.1, and 4.2, respectively. A Ni–Al LDH reference compound was synthesized by controlled hydrolysis (Taylor, 1984). Twenty millimolar $Ni(NO_3)_2$ and 10 m*M* of $Al(NO_3)_2$ were separately titrated up to pH 6.9 using 2.5 *M* NaOH, and then combined by continuous addition of 2.5 *M* NaOH with a pH-stat, the pH of the suspension was maintained at 6.9 for 5 h. The resulting precipitate was collected by centrifugation, washed with deionized water in five cycles, and then freeze-dried. An α-Ni hydroxide reference compound was synthesized by adding 550 mL of 30% ammonia to 500 mL of 1 *M* $Ni(NO_3)_2$ (Génin et al., 1991). After vigorously stirring for 2 h the precipitate was washed and dried as described above. The synthesized precipitates were identified as Ni–Al LDH and α-Ni hydroxide by x-ray diffraction and Fourier transform infrared spectroscopy (Scheinost et al., 1999; Scheinost and Sparks, 2000).

Nickel Sorption Studies

Sorbents were suspended in 0.1 *M* $NaNO_3$ background electrolyte and equilibrated for 24 h, then adjusted to pH 7.5 by addition of 0.1 *M* NaOH or 0.1 *M* HNO_3. Next, 0.1 *M* $Ni(NO_3)_2$ solution was mixed with sodium citrate or sodium salicylate. After ≥2 h, the Ni-ligand solution was slowly added to the sorbent suspension. The final solid concentration was 20 g L^{-1}. A pH of 7.50 ± 0.01 was maintained by continuous addition of 0.1 *M* NaOH using a pH-stat system (Radiometer, Copenhagen, Denmark). Initial metal and ligand concentrations were 1.5 m*M* Ni(II), up to 3 m*M* citrate, and up to 1.5 m*M* salicylate. The suspensions were vigorously stirred and purged with N_2 gas to exclude CO_2. Thirty milliliters of suspension were collected periodically and centrifuged at 27 000 *g* for 3 min to separate wet pastes from solution. The pastes were washed once with background electrolyte and stored in a refrigerator for a maximum of 3 d before collecting DRS spectra. However, to prevent aging effects, the spectra of short-term samples (<24 h) were collected immediately. Supernatants were filtered through a 0.2-μm membrane filter and analyzed for Ni, Al, and Si by inductively coupled plasma atomic emission spectroscopy. Citrate and salicylate were determined with a dissolved organic C analyzer (URA-106, Shimadzu Scientific, Kyoto, Japan). Amounts of sorbed Ni, citrate, and salicylate were calculated from the difference between initial and final concentrations in solution.

Diffuse Reflectance Spectroscopy Studies

The DRS experiments were conducted with a Perkin-Elmer double-beam Lambda 9 spectrophotometer equipped with a Spectralon-coated integrating sphere 5 cm in diameter (Perkin-Elmer, Norwalk, CT). Spectra were collected from 1000 to 500 nm (1-nm steps, 60 nm min^{-1} scan speed, 2-s response time). The wet pastes were filled in an aluminum holder coated with parafilm, 10 mm in diameter and 1 mm in depth, and the surface of the paste was covered with a microscope cover slide. The reflectance was calibrated against a Spectralon standard (Labsphere, North Sutton, NH) covered with another slide to compensate for the absorbance of the glass. The spectra were ratioed against those of blanks; that is, the minerals were prepared the same way as the sorption samples but without Ni or citrate addition. The resulting reflectance spectra were converted into absorbance using the Kubelka–Munk equation, then the $\nu 2$ band positions of the spectra were determined by deconvolution with Gaussian line shapes using GRAMS/32 ver.4.2 (Galactic Industries Corp., Nashua, NH). Detailed procedures are described in Scheinost et al. (1999).

Preparation of Model Mixtures

To calibrate the $\nu 2$ band positions for the quantification of surface precipitates consisting of mixtures of Ni–Al LDH and α-Ni hydroxide, we prepared physical mixtures of freeze-dried Ni–Al LDH and α-Ni hydroxide samples. The DRS analysis of these samples was conducted on dry powders to prevent chemical reactions.

RESULTS AND DISCUSSION

Nickel Sorption Kinetics

Figure 1a shows the influence of citrate on Ni sorption by LS-gibbsite. Without citrate, a fast initial sorption step (<100 h) is followed by a slow step continuing for >1 mo. With increasing citrate the extent of the fast

step decreased, drastically reducing the amount of Ni sorbed at all time steps. This effect is consistent with the complexation of Ni by citrate. Based on the thermodynamic constants of Hedwig et al. (1980), 99% of aqueous Ni occurred as $COH(CH_2COO)_2NiCOO^-$ (at pH 7.5 and 1.5 m*M* citrate). The effect of citrate on Ni sorption depends also on the type of sorbent (Fig. 1b). Without citrate, Ni removal from the solution phase was 99% for pyrophyllite, 97% for HS-gibbsite, but only 53% for LS-gibbsite after 30 d, revealing the dependence of sorption on surface area. In the presence of citrate, however, this sequence changed. While the Ni sorption on LS-gibbsite and pyrophyllite was reduced by 62 and 76%, respectively, citrate reduced the Ni sorption on HS-gibbsite by 5% only. Salicylate, with only one carboxyl group, complexes only ≈25% of aqueous Ni (calculated using the data by El-Ezaby and El-Khalafawy, 1981). As expected, the suppression of Ni sorption by salicylate was weaker than in the presence of citrate (Fig. 1c). Furthermore, with 3% reduction on HS-gibbsite, 8% on pyrophyllite, and 55% on LS-gibbsite, the order of the reduction was different from the Ni–citrate system. The smaller influence of citrate on Ni sorption by the HS-gibbsite than by the LS-gibbsite and the pyrophyllite is in line with the presence of a substantial amount of chemisorbed Ni on HS-gibbsite as has been detected by x-ray absorption fine structure spectroscopy (Yamaguchi and Scheinost, 2000, unpublished data).

Identification of Surface-Induced Precipitates

Figure 2 shows the identification of Ni precipitates by DRS. Fitted $\nu 2$ band positions of the sorption samples are plotted together with gray bands representing the range of Ni–Al LDH and α-Ni hydroxide reference compounds (Scheinost et al., 1999). In the absence of citrate, the $\nu 2$ positions of the LS-gibbsite system increased with time from 15 230 to 15 410 cm^{-1}, but remained in the range indicative of Ni–Al LDH (Fig. 2a). A similar blue shift with aging has been previously observed and explained by crystallite growth (Scheinost et al., 1999). At molar ratios of citrate to Ni of 0.7 and 1 (labeled cit/Ni = 0.7 and 1 in Fig. 2, with Ni = 1.5 m*M*, citrate = 1.0 m*M* and Ni = 1.5 m*M*, citrate = 1.0 m*M*), the $\nu 2$ band was close to the α-Ni hydroxide region, with a slight blue shift with time. For cit/Ni = 0.3, $\nu 2$ was initially in between Ni–Al LDH and α-Ni hydroxide, then dropped down to α-Ni hydroxide, and was up in the Ni–Al LDH range after 30 d. For cit/Ni = 2, the band intensity was too low to reliably determine the band position.

Figure 2b compares band positions of all three sorbents with and without citrate. Without citrate, LS-gibbsite and pyrophyllite induced the formation of Ni–Al LDH. At cit/Ni = 1, a red shift to α-Ni hydroxide was observed in the presence of both HS- and LS-gibbsite, while the precipitate formation was almost completely suppressed for pyrophyllite (the $\nu 2$ band was too weak to be fitted). However, a pyrophyllite sample with a lower citrate/Ni ratio of 0.3 confirms the general trend that increasing citrate causes a red shift of $\nu 2$ positions towards that of α-Ni hydroxide (Fig. 2b).

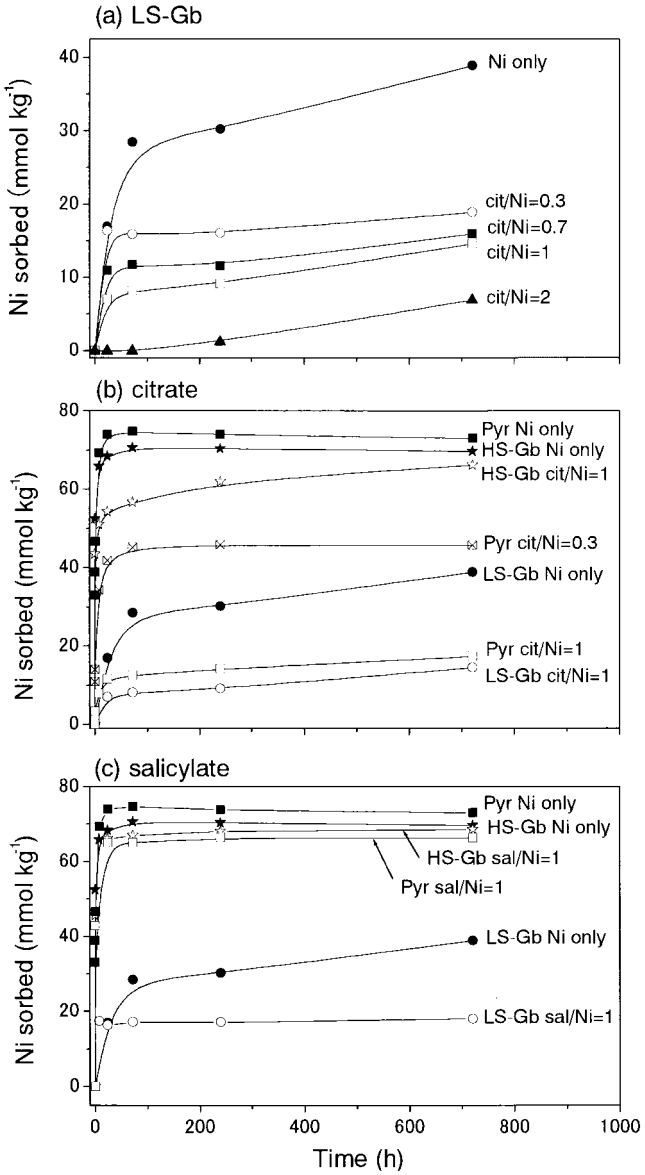

Fig. 1. Influence of ligands on Ni sorption kinetics: (*a*) Ni sorption on low surface area gibbsite with different citrate/Ni ratios; (*b*) Ni sorption on low surface area gibbsite, high surface area gibbsite, and pyrophyllite in the presence and absence of citrate; (*c*) Ni sorption on low surface area gibbsite, high surface area gibbsite, and pyrophyllite in the presence and absence of salicylate.

In the presence of salicylate, the red shift was also observed (Fig. 2c). The $\nu 2$ band positions are predominantly intermediate to those of Ni–Al LDH and α-Ni hydroxide. We assumed that these intermediate positions reflect mixtures of Ni–Al LDH and α-Ni hydroxide. In fact, physical mixtures of both Ni–Al LDH and α-Ni hydroxide showed only one slightly broadened $\nu 2$ band (Fig. 3a). The differing positions of the $\nu 2$ band of Ni–Al LDH and α-Ni hydroxide do not resolve, because they are only 500 cm^{-1} apart, but have a large width at one-half height of ≈4500 cm^{-1}. The fitted positions of this broadened band are intermediate to those of the two single components consistent with the observed band positions (Fig. 3b). Relatively small fractions of α-Ni hydroxide shift the band drastically toward red.

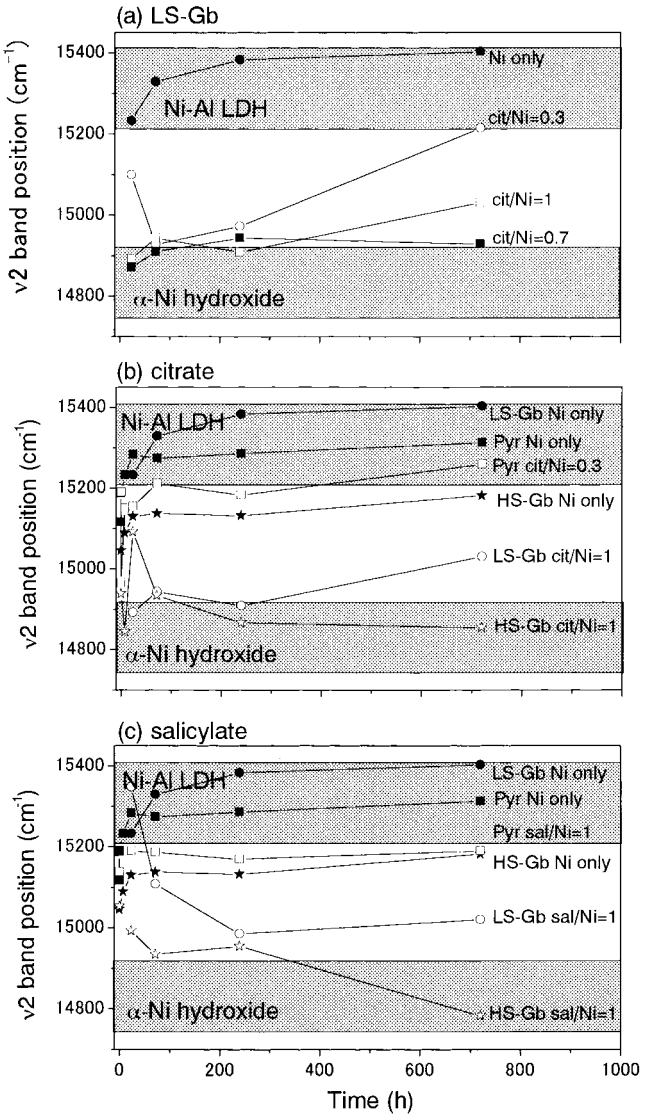

Fig. 2. Influence of ligands on the time-dependent formation of Ni precipitates as investigated by the *v*2 band position: (*a*) Ni sorption on low surface area gibbsite with different citrate/Ni ratios; (*b*) Ni sorption on low surface area gibbsite, high surface area gibbsite, and pyrophyllite in the presence and absence of citrate; (*c*) Ni sorption on low surface area gibbsite, high surface area gibbsite, and pyrophyllite in the presence and absence of salicylate.

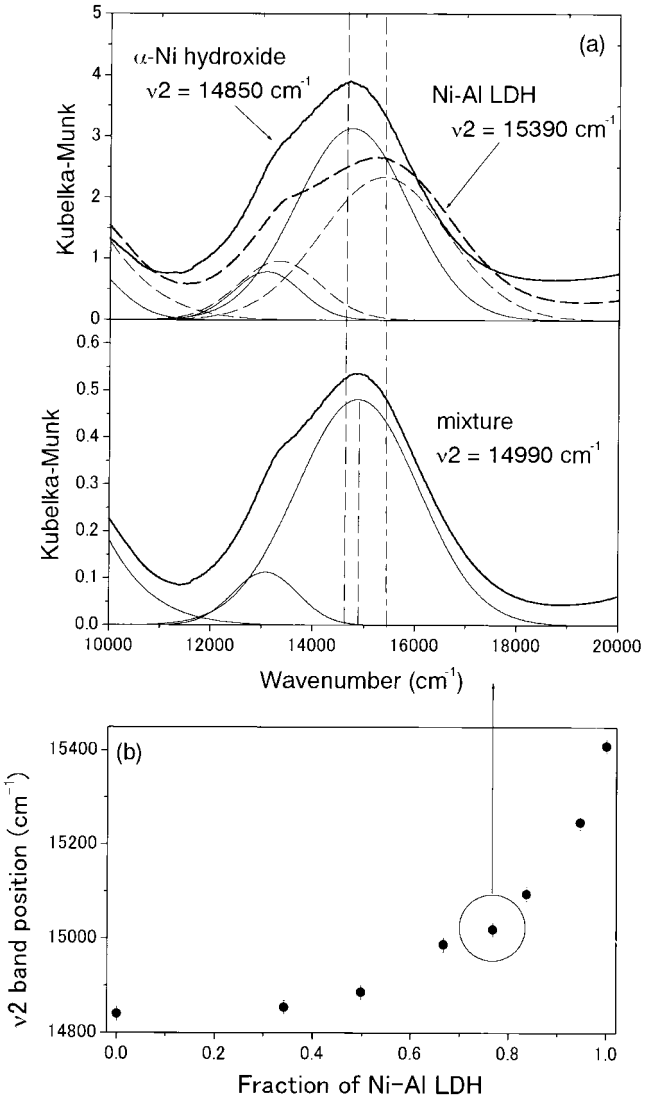

Fig. 3. (*a*) Diffuse reflectance spectroscopy spectrum of Ni–Al layered double hydroxide, α-Ni hydroxide, and physical mixture of α-Ni hydroxide and Ni–Al layered double hydroxide. (*b*) Relationships between *v*2 band position and fraction of α-Ni hydroxide vs. Ni–Al layered double hydroxide.

Kinetics of Citrate and Salicylate Sorption

Figure 4a shows citrate sorption kinetics on LS-gibbsite, HS-gibbsite, and pyrophyllite. The citrate sorption kinetics were similar to those of Ni. The HS-gibbsite sorbed most citrate, followed by LS-gibbsite and pyrophyllite. This sequence is explained by the differences in surface area and surface charge, the latter being positive for gibbsite (PZSE = 9–10) and negative for pyrophyllite (PZSE = 4) at pH 7.5. The presence of Ni reduced the amount of citrate sorbed by gibbsite, but increased the amount of citrate sorbed by pyrophyllite. This can be explained by the reduced negative charge of the Ni–citrate complex (−1) vs. that of citrate (−2 at pH 7.5). At the negatively charged pyrophyllite surface, the less negative charge of Ni–citrate reduces the electrostatic repulsion, thus slightly enhances the probability of Ni–citrate to approach the surface. In contrast, citrate sorption on gibbsite is reduced because the electrostatic attraction between the positively charged gibbsite surface and Ni–citrate is reduced. Furthermore, the single free carboxyl group of Ni–citrate has a much smaller statistical probability of approaching the gibbsite surface in a sterically favorable way to form a surface complex, as compared with the three reactive carboxyl groups of citrate.

In contrast to citrate, most salicylate was sorbed by LS-gibbsite, followed by HS-gibbsite and then by pyrophyllite (Fig. 4b). The presence of Ni did not affect the sorption of salicylate by HS-gibbsite and pyrophyllite, but slightly decreased salicylate sorption by LS-gibbsite. This latter effect is probably caused by the small surface area of LS-gibbsite. At our reaction conditions, salicylate has a higher affinity for Al than for Ni to form

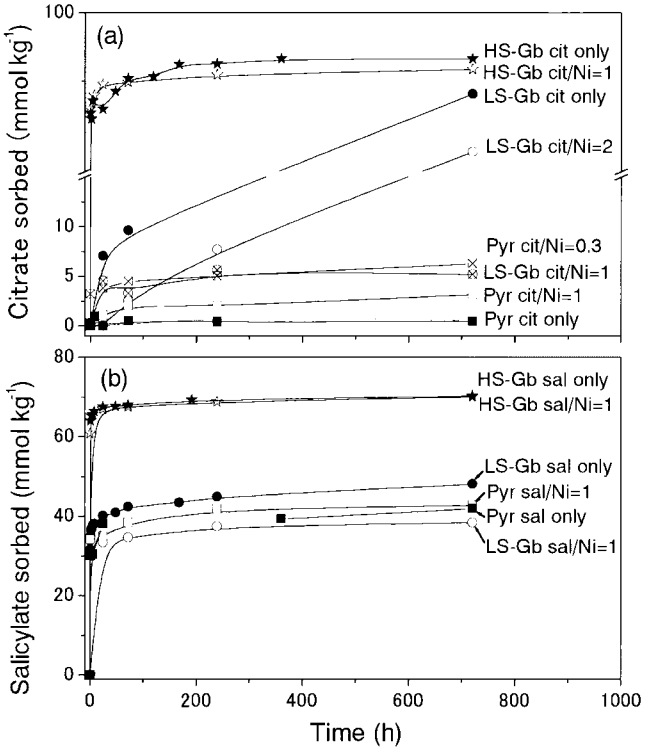

Fig. 4. (*a*) Citrate and (*b*) salicylate sorption on low surface area gibbsite, high surface area gibbsite, and pyrophyllite.

aqueous complexes (based on calculation using MINEQL ver. 4.0; Environmental Research Software, Hallowell, ME). Consequently, salicylate most likely has a smaller affinity for a Ni-covered surface than for a clean Al surface. At the 25% smaller surface area of LS-gibbsite Ni may then out-compete salicylate during sorption.

Aluminum and Silicon Dissolution Kinetics

In the presence of citrate, the Al concentration in solution increased to more than 100 μmol L^{-1} (Fig. 5a). This high Al concentration is caused by citrate-promoted pyrophyllite dissolution, and the subsequent formation of aqueous Al–citrate complexes, which lower the activity of free Al^{3+} and consequently its tendency to form Al hydroxide. The addition of Ni lowered the Al concentration in solution. This may be explained by Al and Ni both competing for citrate complexes, which increases the relative amount of uncomplexed Al and reduces the amount of free citrate available for dissolution of pyrophyllite. Al concentration decreased in the sequence: pyrophyllite ≫ LS-gibbsite > HS-gibbsite (Fig. 5b), corresponding with the sequence in which citrate suppressed the sorption of Ni. This confirms that the suppression mechanism of Ni sorption by citrate is related to Al dissolution. In spite of the fact that little citrate was sorbed on the pyrophyllite surface, Al dissolution was strongly promoted by the presence of citrate. While the addition of Ni suppressed the Al dissolution from the pyrophyllite surface, Si dissolution was not affected (Fig. 5c). Scheidegger et al. (1997) found that Si was dissolved from the pyrophyllite surface by 0.1 *M*

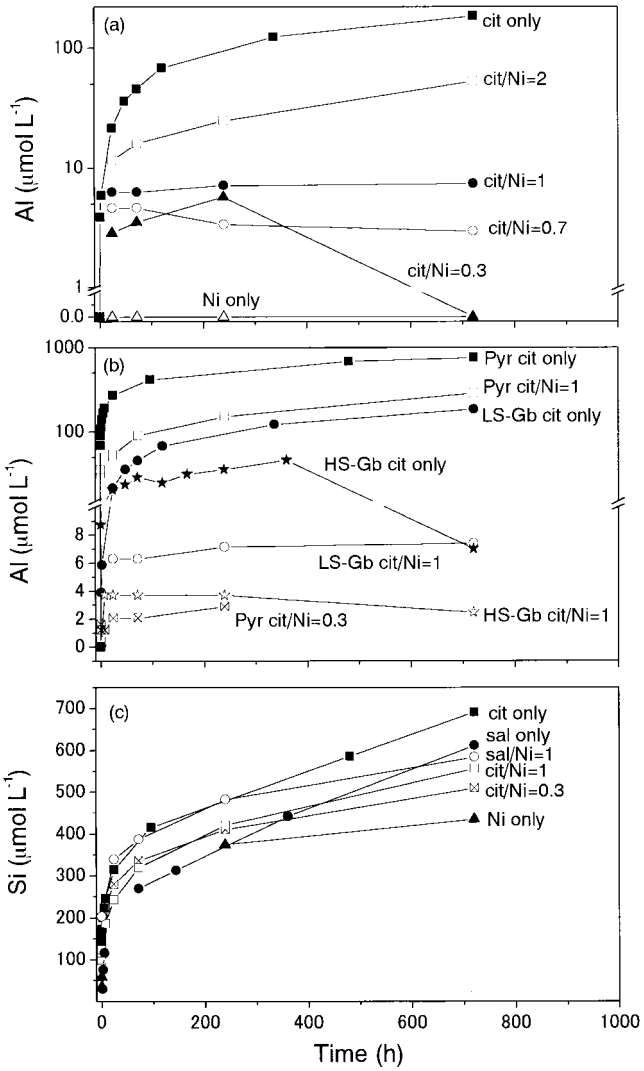

Fig. 5. Influence of Ni and ligands on the Al release from sorbents: (*a*) Al release from low surface area gibbsite at different citrate/Ni ratios; (*b*) Al release from low surface area gibbsite, high surface area gibbsite, and pyrophyllite in the presence of citrate; (*c*) Al and Si dissolution kinetics from pyrophyllite.

$NaNO_3$ at pH 7.5, whereas Al was not detectable. This is due to the low solubility of Al at pH 7.5, causing the Al detached from the pyrophyllite structure to reprecipitate as Al hydroxide (Thompson et al., 1999). While citrate is able to keep more Al in solution by forming an Al–citrate complex, the competitive formation of Ni–citrate complexes reduces the Al solubility in the presence of Ni. Al was not dissolved from gibbsite or pyrophyllite in the presence of salicylate at pH 7.5, neither with nor without Ni. This is in line with results by Kraemer et al. (1998) showing that the salicylate-promoted dissolution of δ-Al_2O_3 had a minimum at pH 7.50. Likewise, the presence of salicylate had no effect on Si dissolution from pyrophyllite.

Mechanisms of Precipitate Formation in the Presence of Ligands

In a homogeneous solution, supersaturation is required to overcome the energy barrier to form crystal-

line nuclei. At [Ni] = 1.5 m*M* and ionic strength *I* = 0.015 *M*, the solution is saturated with respect to Ni–Al LDH above pH 8.1 (solubility products, Ksp = $10^{-26.09}$, Boclair and Braterman, 1999). However, DRS clearly showed the formation of Ni–Al LDH. Likewise, a recent study by Mattigod et al. (1997) showed that saturation with respect to α-Ni hydroxide was achieved at pH 7.50 and [Ni] > 3 m*M*. Therefore, our system was also undersaturated with respect to α-Ni hydroxide. Nevertheless, DRS confirmed that this phase formed in the presence of gibbsite. Our results are in agreement with several other studies, showing that the formation of precipitates at the mineral–water interface occurs under conditions that are undersaturated with respect to the homogeneous solution (Fendorf et al., 1992; Xia et al., 1997). This precipitation may be explained by the combination of several processes. First, the electric field of the mineral surface attracts Ni ions through adsorption, leading to a local supersaturation at the mineral–water interface. Second, the solid phase may act as a nucleation center for polyhydroxy species and catalyze the precipitation process (McBride, 1994, p. 154). Third, the physical properties of water molecules adsorbed at the mineral surface are different from those of free water (Sposito, 1984), potentially causing a lower solubility of metal hydroxides at the mineral–water interface.

Layered double hydroxides are commonly synthesized by the addition of base to a mixture of M(II) and M(III). For the formation of LDH, the M(III) hydroxide that precipitates first must be sufficiently soluble, and the M(II) hydroxide that precipitates second must be sufficiently insoluble (Boclair and Braterman, 1999). Consequently, Al hydroxide is a necessary precursor for the formation of Ni–Al LDH. Our solution data as well as those of Scheidegger et al. (1996, 1997, 1998) and Scheinost et al. (1999) show a substantial Si release from pyrophyllite, indicating the dissolution of this mineral. Although one would expect that the pyrophyllite dissolution leads to a congruent release of Al and Si, Al concentration was below the detection limit in all experiments cited. Since the detection limit for Al in the references cited was above the saturation of amorphous Al hydroxide, it is very likely that the missing Al from pyrophyllite dissolution was precipitated as such an amorphous Al hydroxide.

This explanation is in line with the observed difference between pyrophyllite and gibbsite. While the formation of Ni–Al LDH is rapid on pyrophyllite (≥5 min), it is slow on gibbsite (≥1 d) (Scheidegger et al., 1996, 1997, 1998; Scheinost et al., 1999). Our sorption experiments with citrate, which keeps Al in solution, showed that more Al was dissolved from pyrophyllite than from gibbsite (Fig. 5b), making evident that pyrophyllite is more soluble than gibbsite. Therefore, the dissolution of pyrophyllite produces a substantial amount of amorphous, easily soluble Al hydroxide precipitate, which is responsible for the fast formation of Ni–Al LDH. In contrast, the lower solubility of gibbsite prevents both the immediate reaction of this crystalline Al hydroxide with Ni to form Ni–Al LDH, as well as the formation of a sufficient amount of secondary Al hydroxide. Therefore, the formation of Ni–Al LDH on pyrophyllite and the formation of α-Ni hydroxide on gibbsite give clear evidence that the kinetics of Ni–Al LDH formation is controlled by the solubility of Al from sorbent phases. Due to the higher thermodynamic stability of Ni–Al LDH, however, α-Ni hydroxide precipitates transform into Ni–Al LDH as soon as sufficient Al is available.

The reaction scheme outlined above explains the influence of the organic ligands on both the amount and the composition of the surface-induced precipitates. The formation of stable Ni–organic complexes reduces the formation of Ni hydroxide, which is either the end product of the surface precipitation (α-Ni hydroxide) or the precursor for the subsequent formation of Ni–Al LDH in the presence of an amorphous Al hydroxide. Therefore, the organic ligands generally reduce the amount of Ni surface precipitates. Furthermore, the organic ligands altered the type of precipitates. In spite of the fact that Al was released into solution from both LS- and HS-gibbsite, the formation of Ni–Al LDH was suppressed by citrate. This, and the fact that citrate kept Al effectively in solution, shows that citrate dissolved the secondary amorphous Al hydroxide and subsequently reduced or prevented the formation of Ni–Al LDH. At the lowest citrate/Ni ratio of 0.3, α-Ni hydroxide formed first on LS-gibbsite, but after 30 d Ni–Al LDH predominated (Fig. 2a). Simultaneous to this phase transformation, Al concentration in solution dropped below the detection limit (Fig. 5a). In contrast to the gibbsite system, however, citrate did not prevent the formation of Ni–Al LDH in the presence of pyrophyllite, although it drastically suppressed its amount. Again, this can be explained with the reaction scheme outlined above. Citrate promotes the dissolution of pyrophyllite, but also reduces formation of the secondary, amorphous Al hydroxide phase. Consequently, formation of Ni–Al LDH is reduced. The precipitation of amorphous Al hydroxide is responsible for the rapid formation of Ni–Al LDH (Taylor, 1984). At low citrate concentration ([Ni] = 1.5 m*M*, [cit] = 0.5 m*M*), Al hydroxide was still available to induce the rapid formation of Ni–Al LDH on pyrophyllite though a part was dissolved by citrate. At citrate/Ni = 1 ([Ni] = [cit] = 1.5 m*M*), Al concentration in solution was very high; hence, amorphous Al hydroxide may not have been present. At this reaction condition, no Ni precipitate was formed on pyrophyllite.

Salicylate may suppress the precipitation of Ni by two mechanisms, the complexation of Ni in the aqueous phase and the formation of an adsorption complex with the mineral surface. At the circum-neutral pH of our study, salicylate most likely forms a monodentate sorption complex with the aluminol surface (Kubicki et al., 2000). This adsorbed salicylate may block the surface of Al hydroxide and subsequently suppress the coprecipitation of Al hydroxide with Ni hydroxide. Therefore, the precipitates were dominated by α-Ni hydroxide (Fig. 2c). At the pyrophyllite surface, which is probably coated by secondary Al hydroxide (Thompson et al., 1999), salicylate should preferentially bind to the sorption sites on this secondary Al hydroxide, therefore re-

ducing the nucleation of Ni hydroxide polymers. The weak affinity of salicylate for Ni could also suppress the approach of Ni to the salicylate-adsorbed Al hydroxide surface. However, because of the relatively high solubility of Al at the pyrophyllite surface, the formation of Ni–Al LDH still dominated.

CONCLUSIONS

The presence of organic ligands generally reduced the sorption of Ni on gibbsite and pyrophyllite by suppressing the formation of surface-induced Ni precipitates. The effect of citrate was more pronounced than that of salicylate. In the presence of pyrophyllite, with and without organic ligands, the precipitate phase was Ni–Al LDH. In the presence of gibbsite, however, the organic ligands increased the relative amount of α-Ni hydroxide. The observed effects could be explained by the ligand-enhanced dissolution of the sorbent phases, the formation of aqueous organo-metal complexes, and the interaction of these complexes with the surfaces. The kinetics of precipitate formation was largely controlled by either the less soluble primary Al hydroxide (gibbsite) or more soluble secondary Al hydroxide (pyrophyllite). Both the suppression of precipitates in general and the trend from more stable Ni–Al LDH towards the less stable α-Ni hydroxide may significantly enhance the availability of Ni in soils compared with systems free of organic ligands.

ACKNOWLEDGMENTS

This research was funded by the Japan Securities Scholarship Foundation. We would like to express our gratitude to Mr. B. C. McCandless, Institute of Energy Conversion, Univ. of Delaware, for his generous assistance with the use of the UV-VIS-NIR spectrometer, and to Dr. N. Ogura and Mr. T. Tsushima, Tokyo Univ. of Agriculture and Technology, for the use of the DOC analyzer. N.U.Y. wishes to express special thanks to Drs. M. Okazaki and S. Miyata, Tokyo Univ. of Agriculture and Technology, for their support of her research at the Univ. of Delaware as a visiting scientist.

REFERENCES

Bradbury, M.H., and B. Baeyens. 1997. A mechanistic description of Ni and Zn sorption on Na-montmorillonite. Part II: Modeling. J. Contam. Hydrol. 27:223–248.

Boclair, J.W., and P.S. Braterman. 1999. Layered double hydroxide stability. 1. Relative stabilities of layered double hydroxides and their simple counterparts. Chem. Mater. 11:298–302.

Boily, J.F., and J.B. Fein. 1996. Experimental study of cadmium-citrate co-adsorption onto α-Al_2O_3. Geochim. Cosmochim. Acta 60: 2929–2938.

Brooks, S.C., and J.S. Herman. 1998. Rate and extent of cobalt sorption to representative aquifer minerals in the presence of a moderately strong organic ligand. Appl. Geochem. 13:77–86.

Bryce, A.L., W.A. Kornicker, and A.W. Elzerman. 1994. Nickel adsorption to hydrous ferric oxide in the presence of EDTA: Effects of component addition sequence. Environ. Sci. Technol. 28: 2353–2359.

d'Espinose de la Caillerie, J.B., M. Kermarec and O. Clause. 1995. Impregnation of γ-alumina with Ni(II) or Co(II) ions at neutral pH: Hydrotalcite-type coprecipitate formation and characterization. J. Am. Chem. Soc. 117:11471–11481.

Drever, J.I., and L.L. Stillings. 1997. The role of organic acids in mineral weathering. Colloids Surf. A—Physicochem. Engineer. Aspects 120:167–181.

El-Ezaby, M.S., and T.E. El-Khalafawy. 1981. Complexes of Vitamin B6–IX. Ternary complexes of Ni(II), Cu(II) and Zn(II) with pyridoxamine and salicylic acid. J. Inorg. Nucl. Chem. 43:831–837.

Fendorf, S.E., D.L. Sparks, M. Fendorf, and R. Gronsky. 1992. Surface precipitation reactions on oxide surfaces. J. Colloid Interface Sci. 148:295–298.

Ford, R.G., and D.L. Sparks. 2000. The nature of Zn precipitates formed in the presence of pyrophyllite. Environ. Sci. Technol. 34:2479–2483.

Gadd, G.M. 1999. Fungal production of citric and oxalic acid: Importance in metal speciation, physiology and biogeochemical processes. Adv. Microbial Physiol. 41:47–92.

Génin, P., A. Delahaye-Vidal, F. Portemer, K. Tekaia-Elhisissen, and M. Figlarz. 1991. Preparation and characterization of α-type nickel hydroxide obtained by chemical precipitation: Study of the anionic species. Eur. J. Solid State Inorg. Chem. 28:505–518.

Hashi, K., S. Kikkawa, and M. Koizumi. 1983. Preparation and properties of pyroaurite-like hydroxy minerals. Clays Clay Miner. 31: 152–154.

Hedwig, G.R., J.R. Liddle, and R.D. Reeves. 1980. Complex formation of nickel(II) ions with citric acid in aqueous solution: A potentiometric and spectroscopic study. Aust. J. Chem. 33:1685–1693.

Jones, D.L. 1998. Organic acids in the rhizosphere—A critical review. Plant Soil 205:25–44.

Kraemer, S.M., V.Q. Chiu, and J.G. Hering. 1998. Influence of pH and competitive adsorption on the kinetics of ligand-promoted dissolution of aluminum oxide. Environ. Sci. Technol. 32:2876–2882.

Kubicki, J.D., M.J. Itoh, L.M. Schroeter, and S.E. Apitz. 2000. Bonding mechanisms of salicylic acid adsorbed onto illitic clay: An ATR-FTIR and molecular orbital study. Environ. Sci. Technol. 31: 1151–1156.

Kyle, J.H., A.M. Posner, and J.P. Quirk. 1975. Kinetics of isotopic exchange of phosphate adsorbed on gibbsite. J. Soil Sci. 26:32–43.

Mattigod, S.V., D. Rai, A.R. Felmy, and L. Rao. 1997. Solubility and solubility product of crystalline $Ni(OH)_2$. J. Sol. Chem. 26:391–403.

McBride, M.B. 1994. Environmental chemistry of soils. Oxford Univ. Press, New York.

Roberts, D., A.M. Scheidegger, and D.L. Sparks, 1999. Kinetics of mixed Ni–Al precipitate formation on a soil clay fraction. Environ. Sci. Technol. 33:3749–3754.

Scheckel, K.G., A.C. Scheinost, R.G. Ford, and D.L. Sparks. 2000. Stability of layered Ni hydroxide surface precipitates—A dissolution kinetics study: Geochim. Cosmochim. Acta. 64:2727–2735.

Scheidegger, A.M., G.M. Lamble, and D.L. Sparks. 1996. Investigation of Ni sorption on pyrophyllite: An XAFS study. Environ. Sci. Technol. 30:548–554.

Scheidegger, A.M., G.M. Lamble, and D.L. Sparks. 1997. Spectroscopic evidence for the formation of mixed-cation hydroxide phases upon metal sorption on clays and aluminum oxides. J. Colloid Interface Sci. 186:118–128.

Scheidegger, A.M., D.G. Strawn, G.M. Lamble, and D.L. Sparks. 1998. The kinetics of mixed Ni–Al hydroxide formation on clay and aluminum oxide minerals: A time-resolved XAFS study. Geochim. Cosmochim. Acta 62:2233–2245.

Scheinost, A.C., R.G. Ford, and D.L. Sparks. 1999. The role of Al in the formation of secondary precipitates on pyrophyllite, gibbsite, talc, and amorphous silica: A DRS study. Geochim. Cosmochim. Acta 63:3193–3203.

Scheinost, A.C., and D.L. Sparks. 2000. Formation of layered single- and double-metal hydroxide precipitates at the mineral/water interface: A multiple-scattering XAFS analysis. J. Colloid Interface Sci. 223:167–178.

Schulthess, C.P., and D.L. Sparks. 1986. Backtitration technique for proton isotherm modeling of oxide surfaces. Soil Sci. Soc. Am. J. 50:1406–1411.

Sposito, G. 1984. The surface chemistry of soils. Oxford Univ. Press, New York.

Strom, L. 1997. Root exudation of organic acids: Importance to nutrient availability and the calcifuge and calcicole behavior of plants. Oikos 80:459–466.

Taylor, R.M. 1984. The rapid formation of crystalline double hydroxy salts and other compounds by controlled hydrolysis. Clay Miner. 19:591–603.

Thompson, H.A., G.A. Parks, G.E. Brown, Jr. 1999. Dynamic interactions of dissolution, surface adsorption, and precipitation in an aging cobalt(II)–clay–water system. Geochim. Cosmochim. Acta 63:1767–1779.

Towle, S.N., J.R. Bargar, G.E. Brown, Jr., and G.A. Parks. 1997. Surface precipitation of Co(II) (aq) on Al_2O_3. J. Colloid Interface Sci. 187:62–82.

Xia, K., A. Mehadi, R.W. Taylor, and W.F. Bleam. 1997. X-ray absorption and electron paramagnetic resonance studies of Cu(II) sorbed to silica: Surface-induced precipitation at low surface coverages. J. Colloid Interface Sci. 185:252–257.

Sensitivity of Soil Manganese Oxides: Drying and Storage Cause Reduction

Donald S. Ross,* Heidi C. Hales, Grace C. Shea-McCarthy, and Antonio Lanzirotti

ABSTRACT

Effects of sample treatment must be well understood to avoid artifacts during analysis. The effect of drying and storage was examined on nine medium- to high-Mn aerobic soils using extractable Mn(II), the Cr Oxidation Test, estimated soluble C, and XANES spectroscopy. Long-term storage (430 d) at 3°C had little effect on the Cr test. Air drying at room temperature (25°C ± 3°C) caused a drop in the Cr test within 24 h, with a further decline to as low as 45% of the original after 72 h, and less than 2% after 264 d. Extractability of Mn with pH 4.8 NH_4OAc increased nearly linearly over the same time period from 0.2 mmol kg^{-1} to as high as 2.3 mmol kg^{-1}. Increases in the absorbance of the extract at 360 nm, an estimate of soluble C, were well correlated within each soil with the increase in Mn(II). Pretreatments to remove soluble organics did not cause any increases in the Cr test of dried samples. Therefore, the loss of Cr oxidizing ability appears to be due to reduction of the oxides, not because of increased reduction of the Cr(VI) formed. No changes in XANES spectra were found after short-term air drying at room temperature, but in the three samples examined after 428 d of drying, the main-edge position had a downward shift of about 1.5 eV, indicating reduction. These results confirm previous findings that studies on the reactivity of soil Mn oxides need to avoid sample drying.

Soil manganese oxide surfaces are important reactive sites that may control the behavior of many metals and organics. Mn oxides are particularly important in affecting the movement of contaminant toxic elements such as Cr, Co, Ni, Pu, and As (Bartlett and James, 1979; Amacher and Baker, 1982; Fendorf and Zasoski, 1992). Additionally, a number of investigations have shown that the oxidation of polyphenols, natural and contaminant, takes place on Mn oxide surfaces (Shindo and Huang, 1982; McBride, 1987; Ulrich and Stone, 1989). Understanding the behavior of Mn oxides in the soil environment is important, but previous work has shown that sample handling, especially drying, may have dramatic effects on Mn behavior (Bartlett and James, 1980). Thus it is essential to first understand the effect of analytical techniques, including sample storage, on the oxides.

Heavy-metal accumulation occurs both in soil Mn oxides (Taylor and Nealson, 1966; Jenne, 1968; McKenzie, 1989) and in marine Mn oxides (Burns and Burns, 1977). Cobalt probably accumulates because of oxidation of adsorbed Co(II) to a less mobile Co(III) (Murray and Dillard, 1979). The mechanism for oxidation of Co(II) by buserite has been examined in detail (Manceau et al., 1997). The mechanism for the "specific" adsorption of other metals, such as Pb and Ni, is not completely clear, but is assumed to be related to similarities in electronic structure and substitution. Recent work has shown strong association of ^{239}Pu on Mn oxides in zeolitic tuff (Duff et al., 1998). In addition to Co, oxidation of Cr(III) (Bartlett and James, 1979), As(III) (Oscarson et al., 1981), and Pu (III/IV) (Amacher and Baker, 1982) has been observed. In the case of Cr and Pu, oxidation results in more mobile and potentially toxic species.

Chromium oxidation has received much attention because of the prevalence of Cr at hazardous waste sites. Fendorf and Zasoski (1992) and Charlet and Manceau (1992) both characterized Cr oxidation on synthetic Mn oxides. The accepted mechanism is adsorption of the Cr(III) cation on the Mn oxide surface followed by electron transfer to Mn via oxygen bridges. The Cr(VI) forms an anion that is released from the surface. This mechanism is consistent with earlier findings that adsorption of added Mn(II) on soil Mn oxides initially blocks Cr oxidation (Ross and Bartlett, 1981). Subsequent increases in Cr oxidation correlated with decreases in the extractability of the added Mn(II), presumably because of auto-oxidation.

The oxidation of phenols and polynuclear aromatics (McBride, 1987; Ulrich and Stone, 1989; Whelan, 1995) by Mn oxides appears to follow a similar mechanism of adsorption followed by electron transfer. The resulting products often polymerize, suggesting a role in the creation of stable humic compounds (Shindo and Huang, 1982; Bartlett, 1990), although some evidence suggests that Mn oxides also lyse humic substances to produce low molecular weight organics (Sunda and Kieber, 1994). Naidja et al. (1998) found that the oxidative polymerization reaction between catechol and synthetic birnessite produced an accumulation of reaction products on the oxide surface.

It has long been known that Mn oxides in soils undergo redox changes in response to sample handling and environmental change (Fujimoto and Sherman, 1945). For example, plant deficiencies or toxicities have

Donald S. Ross and Heidi C. Hales, Dep. of Plant and Soil Sciences, Hills Bldg., Univ. of Vermont, Burlington, VT 05405-0082; Grace C. Shea-McCarthy and Antonio Lanzirotti, Univ. of Chicago/CARS, National Synchrotron Light Source, Brookhaven National Lab., Upton, NY 11973-5000. Received 16 Feb. 2000. *Corresponding author (dross@zoo.uvm.edu).

Published in Soil Sci. Soc. Am. J. 65:736–743 (2001).

Abbreviations: Cr test, standard Cr net oxidation test.